A Cross-Layer Investigation for the Throughput Performance of CSMA/CA-Based WLANs With Directional Antennas and Capture Effect

Li-Chun Wang, *Senior Member, IEEE*, Anderson Chen, *Student Member, IEEE*, and Shi-Yen Huang

***Abstract*—In this paper, we develop a physical/medium-access-control (PHY/MAC) cross-layer analytical model to investigate the throughput performance of the wireless local-area network (WLAN) in a lossy wireless environment. From the PHY-layer perspective, the developed model incorporates the effects of capture and directional antennas, while from the MAC-layer perspective, our approach takes into account the carrier-sense multiple access with collision-avoidance (CSMA/CA) MAC protocol and the effect of the backoff process in the IEEE 802.11 WLAN. We derive explicit analytical expressions for the frame outage and capture probabilities of a directional antenna system in the presence of shadowing and Rayleigh fading. Applying this analysis, we can model the interaction between the PHY and MAC layers more accurately for the infrastructure-based WLAN. The numerical results show that our analytical model can approach that attained by simulations. The proposed cross-layer analytical model not only provides insights into the PHY layer impacts on the throughput of the CSMA/CA MAC protocol but also indicates to how directional antennas can improve the CSMA/CA-based WLAN in terms of antenna beamwidth and the number of radio transceivers.**

***Index Terms*—Capture effect, cross-layer analysis, directional antenna, throughput, wireless local area network (WLAN).**

I. Introduction

THE CARRIER-SENSE multiple access with collision-avoidance (CSMA/CA) medium-access-control (MAC) protocol has been adopted in the IEEE 802.11 wireless local-area network (WLAN) to resolve collisions for multiple users in the common shared wireless channel. Current collision models for the CSMA/CA MAC protocol are both pessimistic and optimistic. From the pessimistic standpoint, frame transmissions in the wireless channel may fail due to signal outage, even if it has only one user. From the optimistic standpoint, although multiple frames are simultaneously transmitted from many different users, one of the transmitted frames may be successfully received if the signal-to-interference-noise ratio (SINR) requirement can be satisfied. According to the so-called capture effect, a MAC protocol can be designed to allow multiple simultaneous transmissions to enhance throughput. Hence, it is important to investigate the performance of the CSMA/CA MAC protocol from a physical/MAC (PHY/MAC) cross-layer perspective.

As the demand for the WLAN services has grown dramatically recently, it becomes a crucial issue to further improve the performance for the CSMA/CA-based WLAN. In the literature, there have been three main research directions for this issue. The first direction is from the MAC-protocol perspective [1]–[6]. The authors in [1] and [2] proposed a dynamic tuning algorithm to adjust the backoff window size according to the traffic load. In addition, a fast backoff procedure was proposed in [3]. Packet-pipeline scheduling [4] and the out-of-band signaling [5] were proposed to reduce the possibility of frame collisions. In [6], a frame-concatenation mechanism was introduced to reduce the protocol overhead. The second research direction to improve the throughput of the CSMA/CA-based WLAN is to incorporate the capture effect [7]–[9]. With capture effect, a user can transmit data, even with other simultaneously transmitting users. The third research direction is to adopt directional or smart antennas in WLAN [10]–[22]. The main objective of these works was to modify the MAC protocol to exploit the advantages of directional or smart antennas. These MAC protocols can be categorized into three types: 1) multiple antennas equipped with one radio transceiver and one network allocation vector (NAV) [10]–[13]; 2) multiple antennas equipped with one radio transceiver, but each antenna is associated with distinct directional NAV (DNAV), and the new MAC protocol is designed to dynamically switch antenna to the desired users [14]–[17]; and 3) multiple antennas and radio transceivers, each of which is also associated with independent NAV [18]–[22]. However, most of these MAC protocols considered only an ideal directional antenna pattern and ignore the effects of capture and frame outage.

To our knowledge, in the context of the IEEE 802.11 WLAN, an analytical throughput model, taking into account of the effects of a practical directional antenna pattern, capture, log-normal shadowing, multipath Rayleigh fading, and the number of radio transceivers is still lacking in the literature. The objective of this paper is to develop such a cross-layer

Manuscript received December 19, 2004; revised December 26, 2005, July 17, 2006, and January 2, 2007. This work was supported in part by the National Science Council and the MOE program for Promoting Academic Excellence of University and Aiming for the Top University and Elite Research Center Development (MOEATU plan) under Grants 91-2219-E-009-016, EX-91-E-FA06-4-4, and 89-E-FA06-2-4. The review of this paper was coordinated by Prof. T. Hou.

The authors are with the Department of Communication Engineering, National Chiao-Tung University, Hsinchu 300, Taiwan, R.O.C. (e-mail: lichun@cc.nctu.edu.tw; mingbing.cm87g@nctu.edu.tw).

Color versions of one or more of the figures in this paper are available online at http://ieeexplore.ieee.org.

Digital Object Identifier 10.1109/TVT.2007.900392

analytical model to accurately evaluate the throughput of the CSMA/CA MAC protocol. In our previously published paper [23], we only briefly showed the proposed analytical model without the verification through simulations. Here, we provide the complete derivation of the PHY/MAC analytical model and the more detailed simulation results. Furthermore, we discuss the impacts of SINR requirement, shadowing parameters, directional antenna gain patterns, and the number of radio transceivers for both the uplink and downlink transmissions.

The rest of this paper is organized as follows. In Section II, we briefly introduce the related works regarding the throughput analysis for the CSMA/CA MAC protocol, with and without the capture effect. Section III describes the radio-channel model and then incorporates the impact of directional antenna into the frame outage probability. In Section IV, we first derive the closed-form expression for the capture probability in a log-normally shadowed Rayleigh fading channel. Then, a cross-layer throughput model of an infrastructure-based WLAN with directional antennas is developed. In Section V, we present numerical results to illustrate the impacts of capture effect and directional antenna on the throughput of the CSMA/CA MAC protocol. Finally, we give our concluding remarks in Section VI.

II. MAC-Layer Throughput Performance: Previous Analysis

The analytical models for evaluating throughput of the CSMA/CA MAC protocol have been proposed in [24]–[33]. Under an error-free channel, the saturation-throughput performance, delay, and dropping frame probability of the CSMA/CA MAC protocol, including the backoff process, and finite retransmission limit, were analyzed in [24]–[26], whereas the performance in nonsaturated condition was inspected in [27] and [28]. The effect of backoff freezing, i.e., a station freezing its backoff counter when the channel turns to busy, was considered in [29]. In [8], [30], and [31], the throughput and delay performance of the CSMA/CA MAC protocol were investigated in the presence of Rayleigh fading, shadowing, and finite retransmission limit, but the impact of frame capture on the backoff process was not considered. The authors of [9] considered the cross-layer interaction between the PHY and MAC layers on the per-user throughput performance in multihop ad hoc networks. Recently, the impacts of various incoming traffic load, packet size, and data transmission rate in imperfect channels were studied in [32] and [33]. However, the evaluation method of the PHY-layer effects of frame outage and capture probabilities was not explicitly expressed in [9], [32], and [33]. Furthermore, the impact of the directional antenna with a more practical gain pattern on the throughput of the CSMA/CA MAC protocol is not considered in [24]–[33].

In Section IV, we will propose a PHY/MAC cross-layer analytical model for the CSMA/CA MAC protocol that extends from [24] to further incorporate the effects of frame capture, outage, and a practical gain pattern of directional antennas on the backoff process in the presence of shadowing and Rayleigh fading. To this end, we first summarize the work of [24] and, then, describe the method of incorporating capture effect in the CSMA/CA protocol.

A. CSMA/CA Backoff Process Without Capture Effect [24]

The backoff process aims to resolve the contention issue when multiple users access a common radio channel. According to the CSMA/CA MAC protocol, all users wait for a random duration before transmission. The waiting time is randomly chosen between zero and the backoff window size. Previous outcomes of channel contention will affect the backoff window size. According to the IEEE 802.11 WLAN, the backoff window size is doubled in the next attempt if a frame is collided in the current attempt. When a frame is successfully transmitted or a new frame requests to send, the backoff window size will be reset to the minimum value.

In [24], the author proposed an analytical model to evaluate the saturation throughput for the CSMA/CA MAC protocol. According to the analytical model in [24], the stationary transmission probability τ can be written as follows:

$$\tau = \frac{2}{1 + W_0 + p_c W_0 \sum_{i=0}^{b-1} (2p_c)^i}. \tag{1}$$

From (1), it is implied that a smaller value of p_c leads to a higher transmission probability (τ). However, a higher transmission probability also results in more collisions. For N contending users, the frame collision probability (p_c) is

$$p_c = 1 - (1 - \tau)^{N-1}. \tag{2}$$

Jointly solving (1) and (2), we can obtain the stationary transmission probability τ for a given N and the range of the backoff window size $(W_0, 2^b W_0)$.

Define the normalized system throughput (S) as the fraction of time that the channel is used to transmit payload successfully. In addition, note that the successful transmission probability (p_s) can be computed as the probability that only one user transmits frame under the condition that at least one user is active, i.e.,

$$p_s = \frac{N\tau(1-\tau)^{N-1}}{p_{\rm tr}} \tag{3}$$

where $p_{\rm tr} = 1 - (1-\tau)^N$ is the probability that at least one user is active.

Hence, the normalized system throughput (S) can be expressed as

$$\begin{aligned} S &= \frac{E[\text{payload transmitted during one slot}]}{E[\text{slot duration}]} \\ &= \frac{p_s p_{\rm tr} E[P]}{(1-p_{\rm tr})\sigma + p_{\rm tr} p_s T_s + p_{\rm tr}(1-p_s) T_c} \end{aligned} \tag{4}$$

where $E[P]$, T_s, T_c, and σ represent the average payload size, average successful transmission duration, average collision duration, and an empty slot time, respectively.

B. CSMA/CA With Capture Effect [8]

In [8], the author extended the model of [24] to incorporate the capture effect. The capture probability $(p_{\rm cap})$ is defined as the probability that the received signal-to-interference ratio (SIR) of a transmitted frame (γ) is higher than a required threshold z_0. That is

$$p_{\rm cap} = \sum_{i=1}^{N-1} R_i \cdot \Pr(\gamma > z_0 | i) \tag{5}$$

where R_i represents the probability of the total $(i+1)$ frames contending for transmissions in the same time slot, i.e.,

$$R_i = \binom{N}{i+1} \tau^{i+1} (1-\tau)^{N-i-1}. \tag{6}$$

In [8], the successful transmission probability with capture effect is then defined as

$$p_s = \frac{N\tau(1-\tau)^{N-1} + p_{\rm cap}}{1-(1-\tau)^N}. \tag{7}$$

Following the remaining steps in [24], the throughput performance of the CSMA/CA with capture effect can be obtained based on the modified successful transmission probability in (7). However, the transmission probability τ in [8] is calculated in a lossless channel based on the Bianchi's method [24], where the effects of frame outage and capture in the PHY layer are not considered in the binary backoff process.

In fact, the frame outage decreases the stationary transmission probability (τ), whereas the capture effect increases it. Therefore, in this paper, we consider both the frame outage and capture effects when evaluating the stationary transmission probability in the binary backoff process. We will show how the frame outage and capture effects influence the transmission probability during the backoff process.

III. PHY-Layer Effects

In the time varying wireless channel, a user may fail to receive the packet in the following two scenarios. First, when the received signal strength of a frame is lower than the required threshold due to large propagation attenuation even without any other contenders, the frame is outage that the probability is denoted by p_o. Second, when the received-signal power of the desired frame $(P_{\rm desired})$ does not exceed the interference power of other $(N-1)$ frames with enough margin, the frame is not captured that the probability is denoted by $p_{\rm nc}$. In this section, we first derive the frame outage probability in a log-normally shadowed Rayleigh fading channel with a practical directional antenna.

A. Radio-Channel Characteristics

In this paper, we consider the common channel effects: path loss, shadowing, and Rayleigh fading [34]. Path loss describes the power attenuation due to the propagation distance (r) between a user and the access point. Usually, path loss is modeled as $r^{-\eta}$, where η is the path loss exponent. Hereafter, we choose $\eta = 4$ in this paper. Shadowing is caused by terrain features and can be characterized by a log-normal random variable $10^{\xi/10}$, where ξ is a Gaussian random variable with zero mean and a standard deviation of σ in decibels. At last, Rayleigh fading characterizes the impact of multipath propagation.

Let P_t be the transmission power of a user and consider the antenna gain $G(\theta)$ with the incident angle θ. Then, the received signal power P_r at an access point can be written as

$$P_r = P_t r^{-4} G(\theta) 10^{\xi/10} x^2 \tag{8}$$

where x is a Rayleigh distributed random variable with unit power and has the probability density function (pdf) as follows:

$$f_X(x) = 2xe^{-x^2}. \tag{9}$$

Let $Y = X^2$. Then, the cumulative density function of Y is

$$F_Y(y) = 1 - e^{-y}. \tag{10}$$

B. Outage Probability

The frame outage probability is evaluated when only one user accesses the wireless channel without other competing users. In this case, the total interference power is zero (i.e., $P_I = 0$), and the frame outage probability can be expressed as

$$\begin{aligned} p_o &= \Pr\{\text{SNR} < z_0\} \\ &= \Pr\left\{\frac{P_t r^{-4} G(\theta) 10^{\xi/10} y}{N_0} < z_0\right\} \\ &= \Pr\left\{y < z_0 \frac{N_0}{P_t} r^4 G(\theta)^{-1} 10^{-\xi/10}\right\} \end{aligned} \tag{11}$$

where z_0 is the required received-SNR threshold, and N_0 is the noise power. In the IEEE 802.11 standards, a WLAN device can adopt different modulation and coding schemes according to channel conditions. To evaluate the effect of different transmission rates on the outage probability, we can apply the required received SNR threshold z_0 in accordance with the selected modulation and coding scheme in (11).

C. Effect of Directional Antenna on Outage Probability

Now, we discuss the impact of directional antennas on the frame outage probability. Let L be the cell radius and denote $\theta_{\rm 3dB}$ the 3-dB beamwidth of the directional antenna. Assume that the users are spatially and uniformly distributed within a cell, and thus, the pdf of the distance (r) and angle (θ) between the user and access point can be given by $f_r(r) = 2r/L^2$,

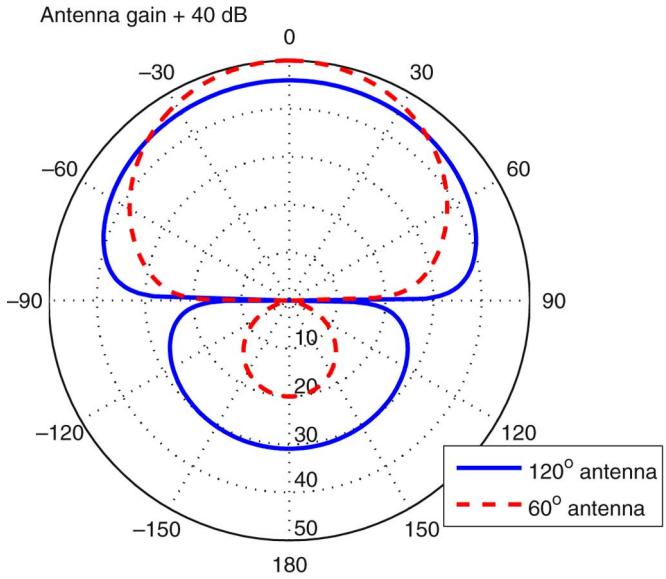

Fig. 1. Examples of antenna-gain pattern for 120° and 60° directional antennas [36], [37].

$f_\theta(\theta) = 1/(2\theta_{3\text{dB}})$, respectively [35]. From (10) and (11), we can have

$$\begin{aligned} p_o &= \Pr\left\{ y < z_0 \frac{N_0}{P_t} r^4 G(\theta)^{-1} 10^{-\xi/10} \right\} \\ &= \int_{-\theta_{3\text{dB}}}^{\theta_{3\text{dB}}} \int_{-\infty}^{\infty} \int_{0}^{L} F_Y\left(z_0 \frac{N_0}{P_t} r^4 G(\theta)^{-1} 10^{-\xi/10} \right) \\ &\qquad \cdot f_r(r) f_\xi(\xi) f_\theta(\theta) dr d\xi d\theta \\ &= \int_{-\theta_{3\text{dB}}}^{\theta_{3\text{dB}}} \int_{-\infty}^{\infty} \int_{0}^{L} \left(1 - e^{z_0 \frac{N_0}{P_t} r^4 G(\theta)^{-1} 10^{-\frac{\xi}{10}}} \right) \\ &\qquad \cdot \left(\frac{e^{-\xi^2/2\sigma^2}}{\sqrt{2\pi}\sigma} \right) \cdot \left(\frac{2r}{2\theta_{3\text{dB}} L^2} \right) dr d\xi d\theta \end{aligned} \quad (12)$$

where $f_\xi(\xi) = e^{-\xi^2/2\sigma^2}/\sqrt{2\pi}\sigma$ represents the distribution of the log-normal shadowing.

Fig. 1 shows two antenna patterns with 3-dB beamwidth of 120° and 60°, respectively [36], [37]. The antenna-gain patterns shown in the figure will be used to evaluate the impact of directional antenna on the MAC-layer throughput later. Note that, inside the 3-dB beamwidth, the gains at different angles are not exactly the same. Therefore, in calculating the outage probability, we need a more practical antenna gain pattern of a sector. Furthermore, it is noteworthy that, for the 120° antenna, the gain at 75° from the main lobe is only about 6 dB less than that in the main lobe. Hence, the antenna gain outside the 3-dB beamwidth cannot be totally neglected, which is especially important in evaluating the capture effect. The impacts of an imperfect antenna on both outage performance and capture effect are not fully considered in the current literature.

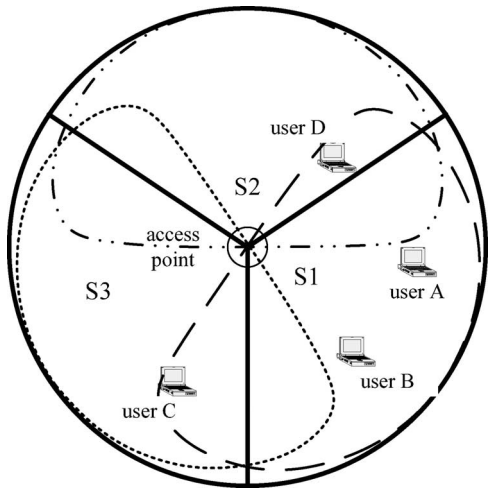

Fig. 2. Coverage pattern of a trisector cell with three 120° directional antennas.

IV. Cross-Layer Throughput Analysis

In this section, we introduce a cross-layer analytical model to evaluate the throughput performance for the CSMA/CA MAC protocol with capture effect and a practical directional antenna. First, we derive the frame-capture probability (p_{cap}) when multiple users transmit frames at the same time. Then, we combine all the wireless channel impacts, including the frame outage, the capture effect, and the gain leakage of a practical direction antenna, to evaluate the throughput of the CSMA/CA MAC protocol.

A. System Model

Fig. 2 illustrates an access point equipped with three directional antennas. A user is usually connected to the sector antenna whose antenna gain is the largest within a cell. In the figure, users A and B communicate with antenna S1, user D communicates with antennas S2, and user C is with antenna S3.

Note that the three directional antennas can share one radio transceiver or can be associated with three independent radio transceivers. In the case with one radio transceiver, the access point can communicate only with one user within a cell by steering the antenna to receive and transmit the signal. On the contrary, in the case with three radio transceivers, the access point simultaneously transmits data frames to three users in three corresponding sectors. For example, if the access point equips with three radio transceivers, users A, C, and D in the figure can simultaneously transmit frames to the access point via antennas S1, S2, and S3, respectively.

B. Capture Effect

Capture effect is the phenomenon that a communication link is established in the presence of other interfering users, while maintaining a satisfactory SINR. Since the interference power is usually higher than the noise power, the SIR is usually used when evaluating the capture probability.

Consider N users (labeled from 1 to N) that are sending the data frames to the access point. The total frame-capture probability ($p_{\text{cap}}(N)$) is defined as [38]

$$p_{\text{cap}}(N) = \Pr\left\{\left(\frac{P_1}{\sum_{i=2}^{N} P_i} > z_0\right) \cup \cdots \cup \left(\frac{P_N}{\sum_{i=1}^{N-1} P_i} > z_0\right)\right\} \tag{13}$$

where z_0 is the required SIR threshold, and P_i is the interference power from user i. Denote the frame-capture probability of user "1" by $p_{\text{cap},1}(N)$. From (8), the received power from user "1" and that from all the interfering users can be written by $P_1 = r_1^{-4} G(\theta_1) 10^{\xi_1/10} y_1$ and $\sum_{i=2}^{N} P_i = \sum_{i=2}^{N} r_i^{-4} G(\theta_i) 10^{\xi_i/10} y_i$, respectively. Thus, it follows that

$$\begin{aligned} p_{\text{cap},1}(N) &= \Pr\left\{P_1 > z_0 \sum_{i=2}^{N} P_i\right\} \\ &= \Pr\left\{y_1 > z_0 \sum_{i=2}^{N} \left(\frac{r_i}{r_1}\right)^{-4} \frac{G(\theta_i)}{G(\theta_1)} 10^{\frac{\xi_i - \xi_1}{10}} y_i\right\}. \end{aligned} \tag{14}$$

Represent $\boldsymbol{r} = (r_2, \ldots, r_N)$, $\boldsymbol{\theta} = (\theta_2, \ldots, \theta_N)$, and $\boldsymbol{\xi} = (\xi_2, \ldots, \xi_N)$ as the distance, angle, and the shadowing components between user $i (i = 2, \ldots, N)$ and the access point, respectively. The frame-capture probability of user "1" for a given $(\boldsymbol{r}, \boldsymbol{\theta}, \boldsymbol{\xi})$ can be expressed as

$$\begin{aligned} &p_{\text{cap},1}(N, r_1, \theta_1, \xi_1 | \boldsymbol{r}, \boldsymbol{\theta}, \boldsymbol{\xi}) \\ &= \int_0^{\infty} \cdots \int_0^{\infty} \exp\left(-z_0 \sum_{i=2}^{N} y_i 10^{\frac{\xi_i - \xi_1}{10}} \frac{G(\theta_i)}{G(\theta_1)} \left(\frac{r_i}{r_1}\right)^{-4}\right) \\ &\qquad \cdot e^{-y_2} \cdots e^{-y_N} dy_2 \cdots dy_N \\ &= \int_0^{\infty} \cdots \int_0^{\infty} \exp\left(-\sum_{i=2}^{N} y_i \left(1 + z_0 10^{\frac{\xi_i - \xi_1}{10}} \frac{G(\theta_i)}{G(\theta_1)} \left(\frac{r_i}{r_1}\right)^{-4}\right)\right) \\ &\qquad \cdot dy_2 \cdots dy_N \\ &= \prod_{i=2}^{N} \frac{1}{1 + z_0 10^{(\xi_i - \xi_1)/10} \frac{G(\theta_i)}{G(\theta_1)} \left(\frac{r_i}{r_1}\right)^{-4}}. \end{aligned} \tag{15}$$

Assume all the interfering users are uniformly distributed in the cell coverage. Averaging over $\boldsymbol{r}$, $\boldsymbol{\theta}$, and $\boldsymbol{\xi}$, the capture probability of user "1" ($p_{\text{cap},1}(N, r_1, \theta_1, \xi_1)$) is

$$\begin{aligned} &p_{\text{cap},1}(N, r_1, \theta_1, \xi_1) \\ &= \int_{-\infty}^{\infty} \int_{-\pi}^{\pi} \int_0^1 \left[\prod_{i=2}^{N} \frac{1}{1 + z_0 10^{(\xi_i - \xi_1)/10} \frac{G(\theta_i)}{G(\theta_1)} \left(\frac{r_i}{r_1}\right)^{-4}}\right] \\ &\qquad \cdot f_r(\boldsymbol{r}) f_\theta(\boldsymbol{\theta}) f_\xi(\boldsymbol{\xi}) d\boldsymbol{r} d\boldsymbol{\theta} d\boldsymbol{\xi} \\ &= \left[\int_{-\infty}^{\infty} \int_{-\pi}^{\pi} \int_0^1 \frac{2 r_i \cdot e^{-\frac{\xi_i^2}{2\sigma^2}} dr_i d\theta_i d\xi_i}{2\pi \cdot \sqrt{2\pi}\sigma \cdot \left[1 + z_0 10^{\frac{\xi_i - \xi_1}{10}} \frac{G(\theta_i)}{G(\theta_1)} \left(\frac{r_i}{r_1}\right)^{-4}\right]}\right]^{N-1}. \end{aligned} \tag{16}$$

To ease illustration, we denote the integral part of (16) by $I(r_1, \theta_1, \xi_1)$, i.e.,

$$I(r_1, \theta_1, \xi_1) = \int_{-\infty}^{\infty} \int_{-\pi}^{\pi} \int_0^1 \frac{2 r_i \cdot e^{-\frac{\xi_i^2}{2\sigma^2}} dr_i d\theta_i d\xi_i}{2\pi \cdot \sqrt{2\pi}\sigma \cdot \left[1 + z_0 10^{\frac{\xi_i - \xi_1}{10}} \frac{G(\theta_i)}{G(\theta_1)} \left(\frac{r_i}{r_1}\right)^{-4}\right]}. \tag{17}$$

Since users 1 to N are assumed to be uniformly distributed and P_i are independent with each other, it can be shown that the average per-user capture probability is the same for all users, i.e., $p_{\text{cap},i}(N) = p_{\text{cap},1}(N)$ for $i = 1$ to N. Averaging over r_1, θ_1, and ξ_1 in (16) to obtain the average per-station capture probability $p_{\text{cap},1}(N)$ and then following the definition in (13), we can obtain the total frame-capture probability for N users $p_{\text{cap}}(N)$ as follows:

$$\begin{aligned} p_{\text{cap}}(N) &= N \cdot \int_{-\infty}^{\infty} \int_{-\theta_{3\text{dB}}}^{\theta_{3\text{dB}}} \int_0^1 p_{\text{cap},1}(N, r_1, \theta_1, \xi_1) \\ &\qquad \cdot f_r(r_1) f_\theta(\theta_1) f_\xi(\xi_1) dr_1 d\theta_1 d\xi_1 \\ &= \int_{-\infty}^{\infty} \int_{-\theta_{3\text{dB}}}^{\theta_{3\text{dB}}} \int_0^1 N \cdot [I(r_1, \theta_1, \xi_1)]^{N-1} \\ &\qquad \cdot \left(\frac{2 r_1}{2\theta_{3\text{dB}}}\right) \cdot \left(\frac{e^{-\frac{\xi_1^2}{2\sigma^2}}}{\sqrt{2\pi}\sigma}\right) dr_1 d\theta_1 d\xi_1. \end{aligned} \tag{18}$$

Note that the integration over the distance in (17) and (18) takes into account of the relative distance from users to the access point, which is in the range (0, 1]. According to [38], the integral in (17) can be simplified as

$$\begin{aligned} &I(r_1, \theta_1, \xi_1) \\ &= \int_{-\pi}^{\pi} \int_{-\infty}^{\infty} \frac{e^{-\frac{\xi_i^2}{2\sigma^2}}}{2\pi \cdot \sqrt{2\pi}\sigma} \cdot \left[1 - r_1^2 \sqrt{z_0 10^{\frac{\xi_i - \xi_1}{10}} \frac{G(\theta_i)}{G(\theta_1)}} \right. \\ &\qquad \left. \cdot \arctan\left(\frac{1}{\sqrt{z_0 10^{\frac{\xi_i - \xi_1}{10}} \frac{G(\theta_i)}{G(\theta_1)}}}\right)\right] \\ &\qquad \cdot dr_i d\xi_i d\theta_i. \end{aligned} \tag{19}$$

Then, applying the Hermite and Gaussian integration method of [34], the integrals, with respect to variables ξ_1 and ξ_i in (18) and (19), can be simplified by a weighted sum of a function evaluated at some roots.

Furthermore, in (17), we also take into account of the interference from all the users in all the three sectors. Because the gain at the angle outside the 3-dB beamwidth cannot be neglected for a practical directional antenna, the interfering users may also be located in neighboring sectors. As shown in Fig. 2, users C and D in sectors S_3 and S_2 may interfere user A

in sector S_1. Therefore, the first integration of $I(\cdot)$ in (17) needs to integrate from $-\pi$ to π, which is different from the case in evaluating the outage probability in (14).

So far, we only focus on the uplink analysis when a user sends packets to the access point. The above analysis can be also extended to the downlink transmission. In the downlink case, $N-1$ users are potential interferers. The capture probability in the downlink case, $p'_{\rm cap}(N)$, can be expressed by

$$p'_{\rm cap}(N) = \Pr\left\{ y_1 > \frac{z_0}{G(\theta_1)} \sum_{i=2}^{N} \left(\frac{r_i}{r_1}\right)^{-4} 10^{\frac{\xi_i - \xi_1}{10}} y_i \right\}. \quad (20)$$

As seen from (20), the role of the directional antenna on the capture effect in the downlink transmission is to increase the signal strength of the desired user. However, in the uplink transmission, not only can the directional antenna increase the signal strength of the desired user, but it can also suppress the interference from other users due to smaller $G(\theta_i)$ in (14) as $|\theta_i|$ increases. Since $p'_{\rm cap}(N)$ in (20) is a special case of $p_{\rm cap}(N)$ in (14), hereafter, we will only consider the capture probability in the uplink transmission.

C. Probability of Packet Loss

Now, we investigate the impacts of frame outage and capture in the PHY layer on the performance of the CSMA/CA MAC protocol. According to [24], the backoff process in the CSMA/CA MAC protocol are mainly characterized by the stationary transmission probability (τ) and collision probabilities (p_c). To establish the cross-layer interaction between the PHY and MAC layers, the probability of packet loss (p_L) is introduced to replace p_c in the pure MAC layer analysis. Specifically, p_L is equal to the sum of the frame outage and noncapture probabilities in the presence of single and multiple users, respectively. That is, for N users, we can write

$$\begin{aligned} p_L(N) &= \Pr\{\text{the channel is bad when only one user intends for transmission}\} \\ &\quad + \Pr\{\text{the signal of the desired user is not captured in the presence of other interfering users}\} \\ &= \sum_{i=1}^{N-1} \binom{N-1}{i} (\tau^*)^i (1-\tau^*)^{N-i-1} \\ &\quad \times (1 - p_{\rm cap}(i+1)) + (1-\tau^*)^{N-1} p_o \quad (21) \\ &\approx (1 - p_{\rm cap}(N)) \sum_{i=1}^{N-1} \binom{N-1}{i} \\ &\quad \times (\tau^*)^i (1-\tau^*)^{N-i-1} + (1-\tau^*)^{N-1} p_o \\ &= (1 - p_{\rm cap}(N)) \left[1 - (1-\tau^*)^{N-1}\right] \\ &\quad + (1-\tau^*)^{N-1} p_o. \quad (22) \end{aligned}$$

As shown in Fig. 3, the total frame-capture probability is insensitive to the number of interfering users N as N increases. This phenomenon is also observed in [38]–[40] through simulations. Thus, in (22), we assume that $p_{\rm cap}(2) = \cdots = p_{\rm cap}(N)$ to reduce the calculation complexity. In Section V, we validate the accuracy of this approximation by OPNET simulation tools.

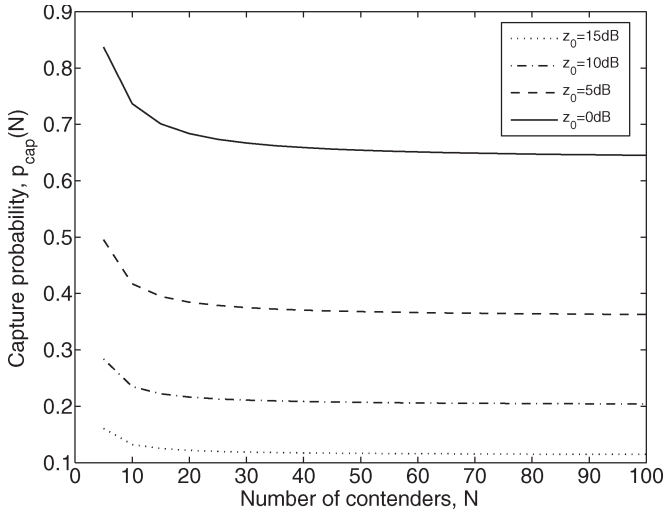

Fig. 3. Relation between the frame-capture probability and number of contending nodes under the 6-dB shadowing standard deviation with different SIR threshold.

At last, replacing p_L with p_c in (1), we rewrite the stationary transmission probability (τ^*) in the PHY/MAC cross-layer analysis as

$$\tau^* = \frac{2}{1 + W + p_L(N) W \sum_{i=0}^{b-1} (2 p_L(N))^i}. \quad (23)$$

D. PHY/MAC Cross-Layer Throughput

The PHY/MAC cross-layer throughput of the CSMA/CA MAC protocol in the composite log-normally shadowed Rayleigh fading channel can be obtained by modifying (4). Incorporating the frame outage probability (p_o) and capture probability $(p_{\rm cap})$ with the stationary transmission probability (τ^*) and its success probability (p_s^*) takes account of the PHY-layer impacts into calculating the MAC-layer throughput.

Consider N users served within an access point. We define n as the effective number of users served by one radio transceiver for an access point equipped with multiple directional antennas. Note that n is dependent of the number of radio transceivers in an access point with multiple directional antennas. For a trisector cell, $n = N$ when the access point has only one radio transceiver, while $n = N/3$ if it is equipped with three radio transceivers. Here, for simplicity, we neglect the contentions from the stations outside the main lobe of a practical directional antenna.

Following (4), the throughput performance $S(n)$ delivered by one radio transceiver can be written by

$$S(n) = \frac{p_{\rm tr}^* p_s^* E[P]}{(1 - p_{\rm tr}^*)\sigma + p_{\rm tr}^* (1 - p_s^*) T_c + p_{\rm tr}^* p_s^* T_s} \quad (24)$$

where $p_{\rm tr}^* = 1 - (1-\tau^*)^n$. Furthermore, in (24), p_s^* is the successful transmission probability in a network, which is a

function of $p_{\rm cap}$ and p_o, i.e.,

$$\begin{aligned} p_s^*(n) &= \frac{1}{p_{\rm tr}^*} \cdot \Pr\{\text{the transmitted frame is captured and not subject to outage}\} \\ &= \frac{1}{1-(1-\tau^*)^n} \\ &\quad \times \left[n\tau^*(1-\tau^*)^{n-1}(1-p_o) \right. \\ &\quad \left. + \sum_{i=1}^{n-1} \binom{n}{i+1} (\tau^*)^{i+1}(1-\tau^*)^{n-i-1} p_{\rm cap}(N) \right] \\ &\approx \frac{1}{1-(1-\tau^*)^n} \left[n\tau^*(1-\tau^*)^{n-1}(1-p_o) \right. \\ &\quad \left. + \left(1-(1-\tau^*)^{n-1}\right) p_{\rm cap}(N) \right]. \end{aligned} \tag{25}$$

Note that the frame-capture probability $p_{\rm cap}(N)$ has to consider the total interference from all the sectors in an access point even when it is equipped with multiple radio transceivers due to the leakage gain of a practical directional antenna. As for the throughput performance for the particular user "i" ($S(n,i)$), (24) can still be reused, where the probabilities $p_{\rm tr}^*$ and $p_s^*(n)$ shall be changed to $p_{\rm tr}^* = \tau^*$, and

$$\begin{aligned} p_s^*(n,i) &= \frac{1}{\tau^*} \left[(1-\tau^*)^{n-1}(1-p_o) \right. \\ &\quad \left. + \left(1-(1-\tau^*)^{n-1}\right) p_{{\rm cap},i}(N) \right] \end{aligned} \tag{26}$$

respectively. The capture probability $p_{{\rm cap},i}(N)$ for user "i" in (26) can be obtained from (16).

To summarize, the PHY/MAC cross-layer throughput of the CSMA/CA MAC protocol can be calculated as follows.

1) Determine the required received SIR threshold (z_0) in (11) and (14) for the corresponding modulation and coding scheme. By choosing an appropriate z_0, the above analysis from (12)–(24) can be applied to the case with different transmission rates.
2) Calculate p_o and $p_{\rm cap}(N)$ for the corresponding z_0 based on (12) and (18), respectively.
3) Find the stationary transmission probability τ^* by substituting p_L of (22) into (23), where $p_{\rm cap}(N)$ and p_o, which are affecting p_L, are calculated in step 2).
4) Determine the effective number of users n according to the number of radio transceivers in an access point.
5) Calculate the successful transmission probability $p_s^*(n)$ by substituting τ^*, p_o, and $p_{\rm cap}(N)$ into (25).
6) Obtain the throughput $S(n)$ of a radio transceiver in a multiple directional antenna system by substituting the stationary transmission probability τ^* and successful transmission probability p_s^* into (24).

The above throughput analysis are suitable for two cases: 1) multiple directional antennas sharing with one NAV and one radio transceiver and 2) multiple directional antennas, each of which has an individual NAV and radio transceiver. It can be applied to the case of multiple directional antennas sharing with one radio transceiver and multiple DNAVs. However, this requires the modeling of the dynamically changing number of effective contending users when switching directional antenna to the desired user based on the detail procedure of the DNAV-based MAC protocol. This is an interesting future research topic but is beyond the current scope of this paper. Nevertheless, we conjecture that the throughput of this DNAV-based MAC protocol will fall between the case of using one radio transceiver with one NAV shared by multiple antennas and that of using multiple radio transceivers with multiple NAVs.

TABLE I
SYSTEM PARAMETERS

MAC header	224 bits
PHY header	192 bits
ACK	304 bits
RTS	352 bits
CTS	304 bits
Bit rate	1Mbit/s
Propagation delay	1μs
Slot time	20μs
SIFS	10μs
DIFS	50μs
Minimum contention window	32
Maximum backoff stage	5
Transmission power, $P_{transmit}$	20 dBm
Noise power, N_0	-90 dBm

TABLE II
REQUIRED SNR THRESHOLD AND OUTAGE PROBABILITY FOR DIFFERENT PACKET LENGTHS

		Antenna type		
Packet length	z_0	Omni-directional	120^o	60^o
60 bytes	-1 dB	0.000685	0.000226	0.0000896
2000 bytes	0 dB	0.000861	0.000284	0.000113

V. NUMERICAL RESULTS

In this section, we present numerical results to compare the throughput performance of the CSMA/CA MAC protocol in WLAN, with and without radio channel impacts. We consider a round coverage area with the radius of 100 m and the shadowing standard deviation equal to 6 dB. In our evaluation, we choose the IEEE 802.11b direct sequence spread spectrum (DSSS) mode for an access point with omnidirectional and directional antennas. Fig. 1 shows the antenna gain patterns of the directional antennas, and Table I lists other system parameters in both the analysis and simulation.

To demonstrate the channel impacts on the required capture threshold, two different packet lengths are studied with the requirement of frame error rate (FER) less than 8×10^{-2} [41]. Table II lists the required received SNR threshold (z_0) and the frame outage probability for the omnidirectional 120° and 60° directional antennas, respectively. A smaller packet of 60 octets requires smaller z_0 and can still achieve the same FER performance as the larger sized 2000 octet packet. Moreover, comparing the frame outage probability for both the omnidirectional- and directional-antenna cases, one can find that the directional antenna can increase the received signal power and, therefore, reduce the frame outage probability.

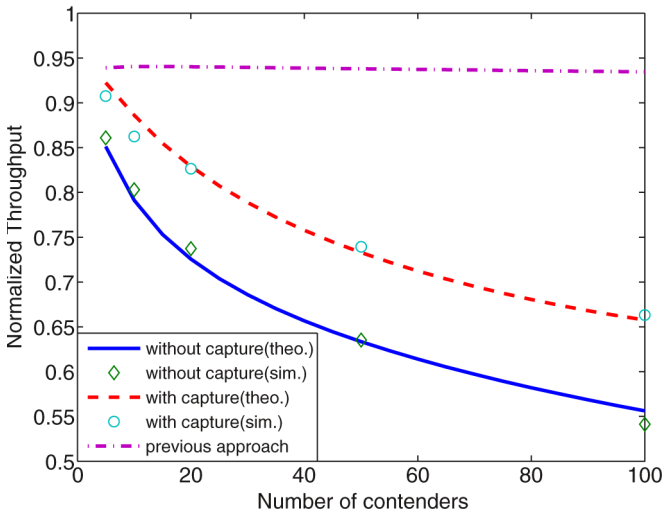

Fig. 4. Capture effect on the throughput of the CSMA/CA MAC protocol with an omnidirectional antenna.

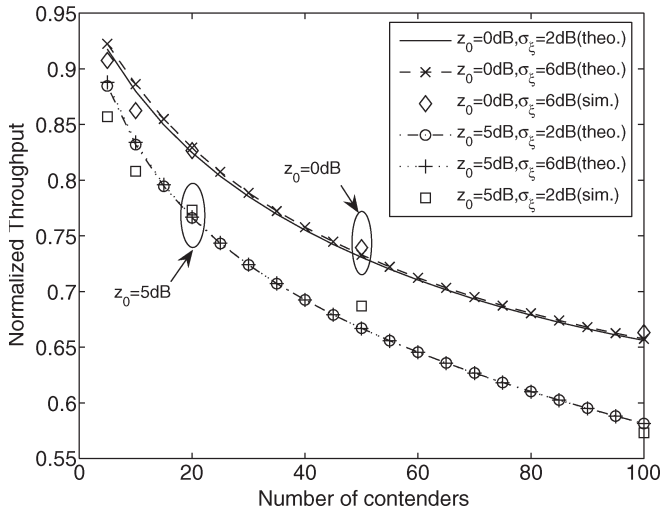

Fig. 5. Shadowing effect on the throughput of the CSMA/CA protocol with various SIR thresholds.

A. *Effect of Large Number of Contenders on Capture Probability*

Fig. 3 shows the frame-capture probability versus the number of contending users with different capture thresholds, where the shadowing standard deviation is 6 dB. We can observe that the capture probability is almost the same when the number of contending users is more than ten. In fact, the phenomenon that the capture probability is insensitive for a large number of stations N can be explained from the derived analytical formulas (16) and (18). Based on (16), the per-station capture probability for user 1 [denoted by $p_{\mathrm{cap},1}(N, r_1, \theta_1, \xi_1)$] decreases as the number of users N increases since there are more interfering users. However, according to (13), as N increases, the total capture probability for N users may also increase because all N users' signals are possibly captured. Combining both the impacts, the average total capture probability $p_{\mathrm{cap}}(N)$ in (18) becomes insensitive to the number of users. This phenomenon is also observed in [38]–[40] by simulations. It helps us to reduce the complexity in the proposed analytical model by using the approximation in (22).

B. *Throughput Comparison for Different Approaches*

Fig. 4 compares the normalized throughput of the CSMA/CA MAC protocol based on different approaches. One can see that, for the case without capture effect, the system throughput degrades severely when the number of users increases. This phenomenon is because frame collisions occur more frequently. For example, when the number of users increases from 50 to 100, the throughput decreases from 0.65 to 0.55. However, the throughput with capture effect only decreases from 0.75 to 0.65 when the number of contenders increases from 50 to 100. Because the capture effect increases the successful transmission probability, the problem of frame collisions can be alleviated. Thus, the throughput performance can be improved, particularly for large number of users.

Note that the improvement resulted from the capture effect is not much when the number of contenders is few. In this situation, the concurrent transmissions are so few that the performance improvement due to the capture effect is insignificant. However, based on the previous approach in [8], the improvements resulted from the capture effect seems too optimistic. Take $N = 10$ as an example. The throughput is about 0.8 in the case without capture, while the throughput based on the previous approach in [8] is 0.94. This is because the capture effect and frame outage is inherently assumed to be independent of the backoff window size in [8], thereby causing the overestimate of the throughput performance. Based on our analytical model, the throughput is 0.85 for $N = 10$, which provides a more reasonable evaluation.

Meanwhile, to validate the accuracy of our proposed analytical model, we also use OPNET simulation to verify the throughput performance in the CSMA/CA MAC protocol. In the simulation, the access point is located in the center of the cell, and all the users are spatially and uniformly located in the cell with radius of 100 m. All the users always transmit frames to the access point with frame length of 2000 bytes. A frame is successfully captured by the access point if the received SIR is larger than the SIR threshold (z_0). The other parameters used in the simulation are listed in Table I. As shown in the figure, both the simulation and analytical results almost match each other, particularly for a large number of users. The discrepancy between the analysis and simulation with small number of users results from the approximation in (22). As shown in Fig. 3, the capture probability does not converge as N is small. Thus, there exists a difference between the exact and approximation values. However, the discrepancy between the analysis and simulation is small, and the developed model still has a certain level of accuracy.

C. *Effect of Shadowing on the Throughput Performance*

Fig. 5 compares the throughput for various shadowing standard deviations ($\sigma_\xi = 2$ and 6 dB) and SIR thresholds ($z_0 = 0$ and 5 dB). As expected, the larger the SIR threshold, the lower the throughput because a more stringent SIR requirement results in more frame errors and higher frame outage probability.

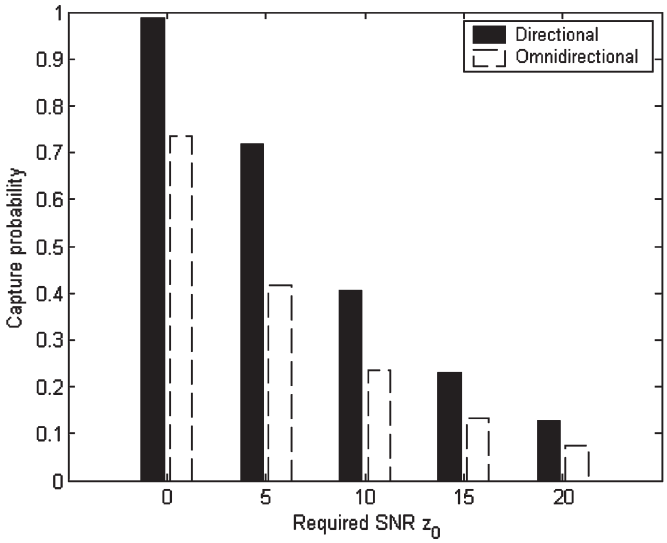

Fig. 6. Comparison of capture effect between omnidirectional and directional antennas.

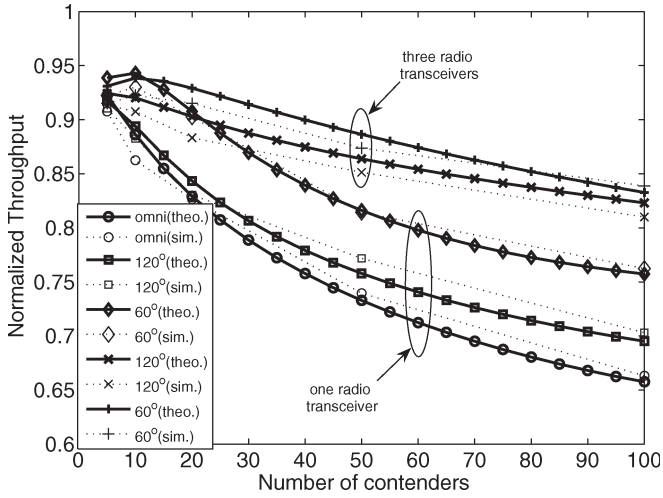

Fig. 7. Effects of multiple directional antenna with single/multiple radio transceivers and channel effects on the throughput of the CSMA/CA protocol.

More interestingly, as shown in the figure, the throughput seemingly does not depend on the shadowing standard deviation. According to (24), the throughput S is determined by the probability of successful transmission p_s^* and stationary transmission τ^*, both of which are dominated by the capture probability. In [35], and [38]–[40], the authors have observed that the capture probability is insensitive to the shadowing parameters but only relates to the SIR threshold. Hence, the phenomenon observed in this paper regarding the shadowing effect on the throughput performance can be justified.

D. Effect of Direction Antennas on Capture Probability

Fig. 6 compares the capture probability of the WLAN system with omnidirectional and 120° directional antennas. Obviously, higher requirement on the received SIR decreases the capture probability for both the omnidirectional and directional cases. However, for the directional-antenna case, the coverage area of an access point is divided into three sectors. Hence, the number of interfering users in a sector is less than that in an omnidirectional-antenna case. As a result, for the same capture probability, the required SIR for the directional-antenna case is about 5 dB less than that in the omnidirectional-antenna case. The improvement for the capture probability between omnidirectional and 120° directional antennas approximates to the reduction ratio for the number of users in one sector (i.e., $10\log(3) = 5$ dB).

E. Effect of Directional Antenna on Throughput Performance

Fig. 7 shows how different kinds of directional antennas affect the throughput of the CSMA/CA MAC protocol. We consider a trisector access point, and each sector is equipped with a 60° or 120° directional antenna, respectively. In addition, two node configurations in the access point are considered: one with a single radio transceiver shared by three antennas and the other with three individual radio transceivers. From (24), the throughput performance $S(n)$ counts the information bits delivered by one radio transceiver. Thus, the performance in the figure for the case of multiple radio transceivers represents the throughput of a single sector, whereas, for the single-transceiver case, it is the overall cell throughput.

For the case with one shared radio transceiver and the number of users $N = 100$, the normalized throughput is 66%, 70%, and 76% for the omnidirectional antenna, 120° and 60° directional antennas, respectively. Compared to the omnidirectional antenna, the interference imposed at the angle of the sidelobe of a directional antenna is lower due to a smaller antenna gain. Moreover, a directional antenna usually has higher antenna gain in the main lobe than an omnidirectional antenna. Therefore, the throughput performance of an access point with a directional antennas is higher than the throughput over the omnidirectional access point, even with one radio transceiver.

Note that, with three radio transceivers, the throughput of a single section can be further improved to 83% and 85% for 120° and 60° directional antennas, respectively. In the case of using multiple radio transceivers, the network is equivalent to one in which the coverage is divided into multiple independent sectors, thereby lowering the number of contenders per radio transceiver and decreasing collisions.

In Fig. 7, we also illustrate both the simulation and analytical results. In the simulation, the access point equips with three directional antennas with the gain patterns shown in Fig. 1. Due to the imperfect antenna-gain pattern, in the simulation, the users in the region outside the main lobe may contend with that inside the main lobe, whereas the developed model neglects these users. Therefore, the contentions from the users in the sidelobe and backlobe result in the discrepancy between the simulation and analytical results.

VI. Conclusion

In this paper, we have developed a PHY/MAC cross-layer analytical model to take account of the PHY layer effects, including the capture effects and a practical directional antenna, into the throughput evaluation of the CSMA/CA MAC protocol. We have derived explicit expressions for the frame outage

and capture probability of a directional antenna system in the presence of log-normal shadowing multipath Rayleigh fading. We integrate this PHY layer model with the MAC throughput analytical model of the CSMA/CA protocol. We find that it is crucial to incorporate the channel effects into both the stationary transmission probability and the backoff window size of a station. By doing so, we can model the interaction of the PHY layer effect and the MAC layer throughput more accurately. Through OPNET simulations, we verify the accuracy of the proposed PHY/MAC cross-layer analytical model.

Our results show that the throughput of the CSMA/CA MAC protocol is insensitive to the shadowing parameters but only relates to the SIR threshold. In addition, directional antennas can improve the throughput of up to 10% even with one radio transceiver. If the access point can be equipped with one radio transceiver for each directional antenna, the throughput of a single section can improve up to 20% due to the improved SIR and fewer effective contenders. This paper can be the basis for some interesting research topics, such as the per-station throughput evaluation or the overall throughput of the multiple directional antennas with multiple DNAVs in multihop networks.

REFERENCES

[1] L. Bononi, M. Conti, and L. Donatiello, "Design and performance evaluation of a distributed contention control (DCC) mechanism for IEEE 802.11 wireless local area networks," in *Proc. ACM WOWMOM*, Oct. 1998, pp. 59–67.

[2] F. Calì, M. Conti, and E. Gregori, "IEEE 802.11 protocol: Design and performance evaluation of an adaptive backoff mechanism," *IEEE J. Sel. Areas Commun.*, vol. 18, no. 19, pp. 1774–1786, Sep. 2000.

[3] Y. Kwon, Y. Fang, and H. Latchman, "Fast collision resolution (FCR) MAC algorithm for wireless local area network," in *Proc. IEEE Global Telecommun. Conf.*, Nov. 2002, vol. 3, pp. 2250–2254.

[4] X. Yang and N. H. Vaidya, "Explicit and implicit pipelining for wireless medium access control," in *Proc. IEEE Veh. Technol. Conf.*, Oct. 2003, vol. 3, pp. 1427–1431.

[5] J. W. Tantra, C. H. Foh, and B. S. Lee, "An efficient scheduling scheme for high speed IEEE 802.11 WLANs," in *Proc. IEEE Veh. Technol. Conf.*, Oct. 2003, vol. 4, pp. 2589–2593.

[6] Y. Xiao, "Concatenation and piggyback mechanisms for the IEEE 802.11 MAC," in *Proc. IEEE Veh. Technol. Conf.*, Oct. 2003, vol. 3, pp. 1453–1457.

[7] J. H. Kim and J. K. Lee, " Capture effects of wireless CSMA/CA protocols in Rayleigh and shadow fading channel," *IEEE Trans. Veh. Technol.*, vol. 48, no. 4, pp. 1277–1286, Jul. 1999.

[8] Z. Hadzi-Velkov and B. Spasenovski, " Capture effect in IEEE 802.11 basic service area under influence of Rayleigh fading and near/far effect," in *Proc. IEEE Int. Symp. Pers., Indoor, Mobile Radio Commun.*, Sep. 2002, vol. 1, pp. 172–176.

[9] M. M. Carvalho and J. J. Garcia-Luna-Aceves, "A scalable model for channel access protocols in multihop ad hoc networks," in *Proc. ACM Annu. Int. Conf. Mobile Comput. Netw.*, Sep. 2004, pp. 330–344.

[10] N. S. Fahmy, T. D. Todd, and V. Kezys, "Ad hoc networks with smart antennas using IEEE 802.11-based protocols," in *Proc. IEEE Int. Conf. Commun.*, Apr. 2002, vol. 5, pp. 3144–3148.

[11] J. Yang, J. Li, and M. Sheng, "MAC protocol for mobile ad hoc network with smart antennas," *Electron. Lett.*, vol. 39, no. 6, pp. 555–557, Mar. 2003.

[12] A. Nasipuri, S. Ye, J. You, and R. E. Hiromoto, "A MAC protocol for mobile ad hoc networks using directional antennas," in *Proc. IEEE Wireless Commun. and Netw. Conf.*, Sep. 2000, vol. 3, pp. 1214–1219.

[13] D. Lal, R. Toshniwal, R. Radhakrishnan, D. P. Agrawal, and J. Caffery, Jr., "A novel MAC layer protocol for space division multiple access in wireless ad hoc networks," in *Proc. 11th Int. Conf. Comput. Commun. Netw.*, Oct. 2002, pp. 614–619.

[14] R. R. Choudhury, X. Yang, R. Ramanathan, and N. H. Vaidya, "Using directional antennas for medium access control in ad hoc networks," in *Proc. ACM Annu. Int. Conf. Mobile Comput. Netw.*, Sep. 2002, pp. 59–70.

[15] M. Takai, J. Martin, A. Ren, and R. Bagrodia, "Directional virtual carrier sensing for directional antennas in mobile ad hoc networks," in *Proc. ACM Int. Symp. Mobile ad hoc Netw. Comput.*, Jun. 2002, pp. 183–193.

[16] R. Ramanathan, "On the performance of ad hoc networks with beamforming antennas," in *Proc. ACM Int. Symp. Mobile ad hoc Netw. Comput.*, Oct. 2001, pp. 95–105.

[17] T. ElBatt, T. Anderson, and B. Ryu, "Performance evaluation of multiple access protocols for ad hoc networks using directional antennas," in *Proc. IEEE Wireless Commun. Netw. Conf.*, Mar. 2003, vol. 2, pp. 982–987.

[18] K. Kobayashi and M. Nakagawa, "Spatially divided channel scheme using sectored antennas for CSMA/CA—'Directional CSMA/CA'," in *Proc. IEEE Int. Symp. Pers., Indoor, Mobile Radio Commun.*, Sep. 2000, vol. 1, pp. 227–231.

[19] T. Korakis, G. Jakllari, and L. Tassiulas, "A MAC protocol for full exploitation of directional antennas in ad-hoc wireless networks," in *Proc. ACM Int. Symp. Mobile ad hoc Netw. Comput.*, Jun. 2003, pp. 98–107.

[20] L. Bao and J. J. Garcia-Luna-Aceves, "Transmission scheduling in ad hoc networks with directional antennas," in *Proc. ACM Annu. Int. Conf. Mobile Comput. Netw.*, Sep. 2002, pp. 48–58.

[21] H. Singh and S. Singh, "DOA-ALOHA: Slotted ALOHA for ad hoc networking using smart antennas," in *Proc. IEEE Veh. Technol. Conf.*, Oct. 2003, vol. 5, pp. 2804–2808.

[22] W. T. Chen, M. S. Pan, and J. J. Dai, "An adaptive MAC for wireless ad hoc networks using smart antenna system," in *Proc. IEEE Veh. Technol. Conf.*, Oct. 2003, vol. 5, pp. 2794–2798.

[23] L. C. Wang, S. Y. Huang, and A. Chen, "A cross-layer throughput performance investigation for CSMA/CA-based wireless local area network with directional antennas and capture effect," in *Proc. IEEE Wireless Commun. Netw. Conf.*, Mar. 2004, vol. 3, pp. 1879–1884.

[24] G. Bianchi, "Performance analysis of IEEE 802.11 distributed coordination function," *IEEE J. Sel. Areas Commun.*, vol. 18, no. 3, pp. 535–547, Mar. 2000.

[25] Y. Tay and K. Chua, "A capacity analysis for the IEEE 802.11 MAC protocol," *ACM Wirel. Netw.*, vol. 7, no. 2, pp. 159–171, Mar. 2001.

[26] Y. Xiao, "Saturation performance metrics of the IEEE 802.11 MAC," in *Proc. IEEE Veh. Technol. Conf.*, Oct. 2003, vol. 3, pp. 1453–1457.

[27] K. Duffy, D. Malone, and D. J. Leith, " Modeling of 802.11 distributed coordination function in non-saturated condition," *IEEE Commun. Lett.*, vol. 9, no. 8, pp. 715–717, Aug. 2005.

[28] M. Garetto and C. F. Chiasserini, "Performance analysis of 802.11 WLANs under sporadic traffic," in *Proc. Networking*. New York: Springer-Verlag, May 2005, vol. 3462, pp. 1343–1347.

[29] C. H. Foh and J. W. Tantra, "Comments on IEEE 802.11 saturation throughput analysis with freezing of backoff counters," *IEEE Commun. Lett.*, vol. 9, no. 2, pp. 130–132, Feb. 2005.

[30] P. Chatzimisios, A. Boucouvalas, and V. Vitsas, "EEE 802.11 packet delay—A finite retry limit analysis," in *Proc. IEEE Global Telecommun. Conf.*, Dec. 2003, vol. 2, pp. 950–954.

[31] Z. Hadzi-Velkov and B. Spasenovski, "Saturation throughput—Delay analysis of IEEE 802.11 DCF in fading channel," in *Proc. IEEE Int. Conf. Commun.*, May 2003, pp. 121–126.

[32] M. Ergen and P. Varaiya, "Throughput analysis and admission control for IEEE 802.11a," *Mobile Netw. Appl.*, vol. 10, no. 5, pp. 705–712, Oct. 2005. Springer.

[33] Y. Zheng, K. Lu, D. Wu, and Y. Fang, "Performance analysis of IEEE 802.11 DCF in imperfect channels," *IEEE Trans. Veh. Technol.*, vol. 55, no. 5, pp. 1648–1656, Sep. 2006.

[34] J. P. Linnartz, *Narrowband Land-Mobile Radio Networks*. Boston, MA: Artech House, 1993.

[35] C. T. Lau and C. Leung, "Capture models for mobile packet radio networks," *IEEE Trans. Commun.*, vol. 40, no. 5, pp. 917–925, May 1992.

[36] C. Balanis, *Antenna Theory*. New York: Harper & Row, 1982.

[37] L. C. Wang and K. K. Leung, "A high-capacity wireless network by quad-sector cell and interleaved channel assignment," *IEEE J. Sel. Areas Commun.*, vol. 18, no. 3, pp. 472–480, Mar. 2000.

[38] M. Zorzi and R. R. Rao, "Capture and retransmission control in mobile radio," *IEEE J. Sel. Areas Commun.*, vol. 12, no. 8, pp. 1289–1298, Oct. 1994.

[39] M. Zorzi, " Capture probabilities in random-access mobile communications in the presence of Rician fading," *IEEE Trans. Veh. Technol.*, vol. 46, no. 1, pp. 96–101, Feb. 1997.

[40] B. Hajek, A. Krishna, and R. O. LaMaire, "On the capture probability for a large number of stations," *IEEE Trans. Commun.*, vol. 45, no. 2, pp. 254–260, Feb. 1997.

[41] *Part 11: Wireless LAN Medium Access Control (MAC) and Physical Layer (PHY) Specification*, IEEE Std. 802.11, Nov. 1999.

Li-Chun Wang (S'92–M'96–SM'06) received the B.S. degree in electrical engineering from the National Chiao-Tung University, Hsinchu, Taiwan, R.O.C., in 1986, the M.S. degree in electrical engineering from the National Taiwan University, Taipei, Taiwan, in 1988, and the M.Sc. and Ph.D. degrees in electrical engineering from Georgia Institute of Technology, Atlanta, in 1995 and 1996, respectively.

From 1990 to 1992, he was with the Telecommunications Laboratories, Ministry of Transportation and Communications, Taiwan (currently, the Telecom Laboratories, Chunghwa Telecom Company). In 1995, he was with Bell Northern Research of Northern Telecom, Inc., Richardson, TX. From 1996 to 2000, he was with AT&T Laboratories, where he was a senior technical Staff Member with the Wireless Communications Research Department. Since August 2000, he has been an Associate Professor with the Department of Communication Engineering, National Chiao-Tung University. His current research interests are in the areas of cellular architectures, radio-network resource management, cross-layer optimization, and cooperation wireless-communication networks. He is the holder of a U.S. patent with three more pending.

Dr. Wang was the corecipient (with G. L. Stuer and C.-T. Lea) of the 1997 IEEE Jack Neubauer Best Paper Award for his paper "Architecture design, frequency planning,and performance analysis for a microcell/macrocell overlaying system," which appeared in the IEEE TRANSACTIONS ON VEHICULAR TECHNOLOGY (best systems paper published in 1997 by the IEEE Vehicular Technology Society). He is currently an Associate Editor for the IEEE TRANSACTIONS ON WIRELESS COMMUNICATIONS.

Anderson Chen (S'04) received the B.S. and M.S. degrees in communication engineering from the National Chaio-Tung University, Hsinchu, Taiwan, R.O.C., in 1998 and 1999, respectively, where he is currently working toward the Ph.D. degree in communication engineering with the Department of Communication Engineering.

His current research interests include wireless networks, cross-layer design, and cognitive wireless systems. He is the holder of a U.S. patent with two more pending.

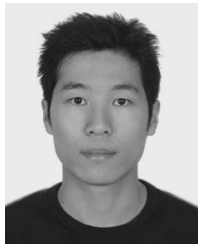

Shi-Yen Huang received the B.S. and M.S. degrees in communication engineering from the National Chiao-Tung University, Hsinchu, Taiwan, R.O.C., in 2001 and 2003, respectively.

He is currently working on his national service and is planning to study for the Ph.D. degree in the future. His research interests include wireless-communication systems and network-performance analysis.